

## THE STUDY OF AN INTERACTION OF SOLID PARTICLES WITH VARIOUS SURFACES USING TSM SENSORS

Qiliang Zhang<sup>1</sup>, Ryszard Lec<sup>1,2</sup> and Kambiz Pourrezaei<sup>1,2</sup>

<sup>1</sup> Department of Electrical and Computer Engineering, Drexel University, Philadelphia, PA 19104

<sup>2</sup> School of Biomedical Engineering, Science and Health System, Drexel University, Philadelphia, PA 19104

**Abstract** - The interaction of solid particles with various surfaces has been experiencing growing interest in the area of nanotechnology, colloidal science and biology. In this paper interactions of solid particles with various surfaces using piezoelectric Thickness Shear Mode (TSM) sensors have been studied. A mechanical model has been presented to evaluate the effect of particle loading on the behavior of a TSM sensor. The main sources contributing to the interaction, such as Van der Waals force, gravitational force and electrostatic force, are discussed. Experimental results have shown that the resonant frequency of a TSM sensor depends on the coupling conditions of micro- or nano- particles loaded on the surfaces of a TSM sensor, which is predicted by the theoretical model. The results show that this TSM sensor technique can provide the information of the coupling, such as the binding energy between the particles and the sensor surfaces, and may promote the applications of TSM sensors in characterizing the properties of the loaded particles.

**Keywords** – Interfacial interaction, particle, TSM, piezoelectric sensor

### I. INTRODUCTION

The study on the interaction of micro/nano objects with various surfaces has attracted growing interest in recent decades [1-6]. Developments of micro and sub-micro electronics and the research on the interactions of biological objects with various functionalized surfaces in the biomedical, biochemical and pharmaceutical industry have been a driving force [7,8].

Understanding of the nature of micro- and nano- world requires broad range measurement techniques and advanced instrumentations to assist the study of the interaction of solid particles with various surfaces. High-resolution optical microscope, scanning electron microscope (SEM) [9] and scanning tunneling microscope (STM) [10] have provided very useful visual information about the surface status and atomic structure of the material. The development of atomic force microscope (AFM) [11] make possible to directly investigate mechanical interactions between objects on the atomic scale. Although AFM has the advantages in both imaging and probing or manipulating micro- and nano-particles, further development of nano-technology requires reliable and cost efficient sensor techniques capable of real-time analysis of the properties of particles or biological objects. In our paper, we study a piezoelectric Thickness Shear Mode (TSM) sensor made of AT-cut quartz crystal as a candidate [12].

Since the pioneer work by G. Sauerbrey in 1950's [13], the characteristics of TSM sensor under different loading has been the topic of many papers. Theoretical equations and simulation models have been developed to study the dependence of the resonant frequency of the TSM sensor on different mechanical loading. The resonant frequency of the sensor has been found to be a function of the properties of the mass layer, such as thickness, density, elastic constant, etc. This has been applied into monitoring thin-film thickness during deposition in the semiconductor industry. Because of the promising potential of TSM sensors in biochemical and biomedical applications, research on the TSM sensor has rapidly spread into the condition of liquid loading with additional mass layer attached to the sensor surface [14,15]. Gas and liquid pressure sensors, viscosity sensors, and latest implantable blood pressure sensor have been reported. Piezoelectric biosensor assays for bacterial toxicity determination in environmental samples has been tested [16].

Recently, the study of the behavior of an assembly and a single cell has been rapidly progressing due to the accelerating growth of tissue engineering. Previous research on the behaviors of the piezoelectric sensors under the load of a solid particle has been very limited [2]. In this paper, based on a mechanical model of a TSM sensor coupling system, the change of the resonant frequency of the sensor has been determined and related to the properties of the particle loading.

### II. Theory

The effects of liquid and/or solid loadings placed on the surfaces of TSM sensors on the behavior of the sensors have been previously studied based on theoretical analysis of different models. G. Sauerbrey derived the equation of the resonant frequency change of TSM sensor due to the mass loading on the surface of TSM sensor [13]. E. Benes presented one-dimension composite resonator model [17]. Stephen Martin and others derived the electrical admittance from a modified Butterworth-Van Dyke equivalent circuit [18]. Many others papers have contribute to the development of the modeling of TSM sensor with different loading. But most of the effort has been focused on the condition that the mass/liquid loaded on the TSM sensor surface is strongly coupled to the sensor, such as a deposited film firmly attached to the surface. The situation that the coupling between the loaded object and the TSM sensor is

relatively weak has not been studied in details. In this paper, an interaction between a solid particle and the surface of a TSM sensor is studied theoretically and experimentally.

#### A. Interaction Forces between a Solid Particle and the Surface of a TSM Sensor

The interest of this paper is focused on the interaction of a solid particle in contact with a TSM sensor in air, as shown in Figure 1.

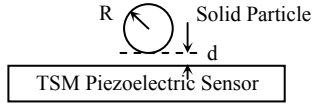


Fig. 1. A solid particle “in contact” with a TSM sensor (R: radius of the particle; d: distance between the particle and the surface)

Fig.2 shows the shear motions of the surface of a TSM sensor coupled with a solid particle.

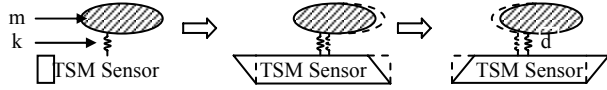


Fig. 2. Shear motions of a TSM sensor coupled with a solid particle (m: mass of the particle; k: coupling constant; d: distance between the particle and the surface)

The interaction forces between a solid particle and the surface of a TSM sensor come from various sources, such as Van der Waals force, friction force, electrostatic force, capillary force and gravitational force, etc.

##### a. Van der Waals force

Van der Waals free energy,  $w(d)$ , and Van der Waals (VDW) force,  $f(d)$ , for a solid particle with the size of tens of nanometers to several hundred micrometers, in contact with a surface can be described by [1]

$$w(d) = -\frac{A \cdot R}{6 \cdot d} \quad \text{and} \quad f(d) = \frac{A \cdot R}{6 \cdot d^2} \quad (1)$$

where  $A$  is Hamaker constant and about  $(0.4 \sim 4) \times 10^{-19}$  J;  $R$ , is the radius of a particle (assume the particle is spherical);  $d$ , is the distance between the particle and the sensor surface, the VDW force is linearly proportional to the radius,  $R$ , of the particle and inversely proportional to the square of the distance of the particle from the surface.

By comparing the VDW force between the particle and the surface of a TSM sensor with the gravity force of the particle, it has been shown in Fig. 3 that the VDW force becomes several orders greater than the gravity force for a nano/micro particle. For example, the VDW force between a particle and a surface is about  $10^7$  times larger than the gravity force for a stainless steel sphere of 1  $\mu\text{m}$  diameter.

##### b. Other forces

Other interaction forces, such as electrostatic force, friction force, capillary force, etc., play a less important role than the VDW force in the interfacial interaction of a solid

particle with the gold surface (electrode) of a TSM sensor *in air* [5]. Under certain conditions, such as proper grounding and discharging of the particle and the sensor, smooth surface of the sensor, low humidity in the air, etc., we can consider Van der Waals force as the dominant interaction between a solid particle and a TSM sensor.

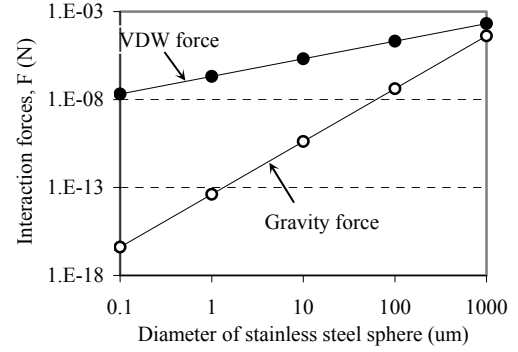


Fig. 3. Comparison between Van der Waals force and gravity force

#### B. Coupling Constant between a Solid Particle and the Surface of a TSM Sensor

The coupling constant,  $k$ , represents the coupling strength of the interaction between a solid particle and a TSM sensor. By knowing the Van der Waals force,  $f(d)$ , the coupling constant,  $k$ , can be estimated by

$$k = -\frac{\partial (F_{vdw})}{\partial d} = \frac{A \cdot R}{3 \cdot d^3} \quad (2)$$

Fig. 4 shows the dependence of the coupling strength,  $k$ , with the diameter, or  $\phi = 2R$ , of the particle.

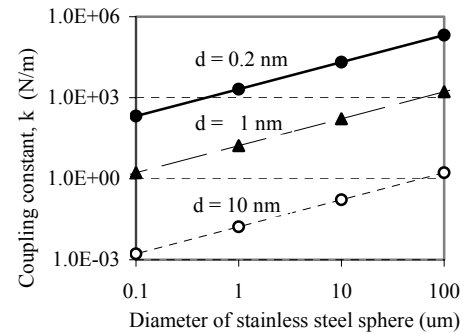


Fig. 4. Coupling constant,  $k$ , as a function of the diameter of a solid particle with different distance,  $d$ , between the particle and the surface

The coupling constant,  $k$ , is linearly proportional to the diameter of a particle but inversely proportional to the cubic of the distance,  $d$ , between a particle and the surface of a TSM sensor.

For a particle of 10  $\mu\text{m}$  diameter *in contact* ( $d = 0.2$  nm, solid line in Fig. 4) with the surface of a TSM sensor, the coupling strength,  $k$ , is about  $10^4$  N/m, which is comparable with the other literature data [2].

#### C. Resonant Frequency of a Solid Particle Coupled with a Solid Surface

A particle placed on a solid surface can be represented as a mechanical resonator. Its resonant frequency can be given as (3).

$$f_p = \frac{1}{2\pi} \sqrt{\frac{k}{m}} = \frac{1}{2\pi} \sqrt{\frac{A}{4\pi \cdot d^3 \cdot R^2}} \quad (3)$$

where,  $m$ , is the mass of the particle;  $k$ , is the coupling constant between the particle and the surface and can be determined by (2).

Fig. 5 shows that the resonant frequency,  $f_p$ , of a coupled particle is inversely proportional to its radius,  $R$ .

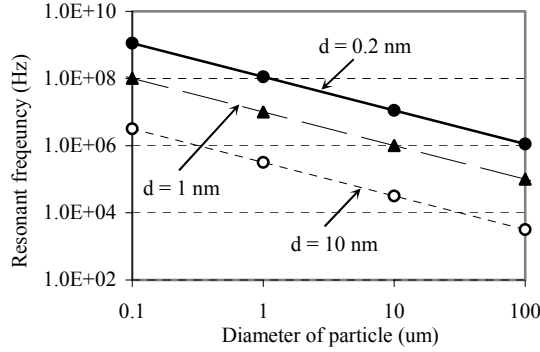


Fig. 5. Resonant frequency of a solid particle coupled with a TSM sensor with different distance,  $d$ , between the particle and the surface

From this figure, it results that the particle can be conveniently interrogated by a TSM sensor. When a solid particle is placed on the surface of a TSM sensor, the interaction between the particle and the TSM sensor can result in changes in the characteristic of the TSM sensor, such as its resonant frequency and resonant amplitude, etc. By monitoring these changes, information about the interaction and some properties of the particle can be obtained.

#### D. Mechanical Model of an Interaction between a Solid Particle and the Surface of a TSM sensor

A mechanical model describing the interaction of a solid particle with the surface of a TSM sensor is proposed in Fig. 6.

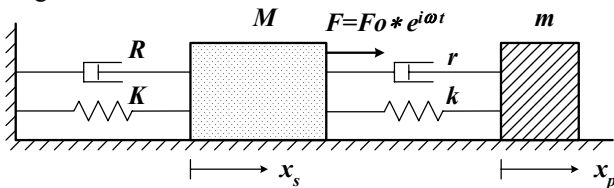


Fig. 6. A mechanical model of an interaction between a solid particle and the surface of a TSM sensor

A piezoelectric TSM sensor is represented by a mechanical resonator consisting of  $M$ ,  $K$  and  $R$ ;  $M$ , is the mass of the TSM sensor and,  $K$ , is the elastic constant of the sensor;  $x_s$ , and  $x_p$ , are the displacements of the surface of a TSM sensor and the coupled particle, respectively;  $R$ , is the

resistive loss factor. The fundamental resonant frequency of the TSM sensor,  $f_s$ , is given as

$$f_s = \frac{1}{2\pi} \cdot \sqrt{\frac{K}{M}} \quad (4)$$

The mass,  $M$ , is driven by a force  $F = F_0 \cdot e^{j\omega t}$ , which is equivalent to an electrical voltage to generate the shear motion of a TSM sensor. The coupled particle is modeled as a rigid mass,  $m$ . The interfacial interaction between the particle and the surface of a TSM sensor is represented by a spring,  $k$ , and a dashpot,  $r$ .

Since a quartz crystal resonator has a very high quality factor,  $Q$ , the energy dissipation of a TSM sensor is very small, i.e.  $R \ll 0.01 \Omega$ . Thus the loss in the operation of the mechanical oscillation (or the oscillation of TSM sensors) can be ignored in most consideration. The energy loss during the interaction mostly comes from the friction force between the particle and the sensor surface. To get a preliminary outlook of the interaction between the particle and the surface, we assume that the mechanical motions in Fig. 6 are lossless,  $R = r = 0$ . Then the equations of motion of the mass,  $M$  and  $m$ , are given as

$$M \cdot \ddot{x}_s + K \cdot x_s - k \cdot (x_p - x_s) = F_0 \cdot e^{j\omega t} \quad (5)$$

$$m \cdot \ddot{x}_p + k \cdot (x_p - x_s) = 0 \quad (6)$$

Assume that the displacements,  $x_s$  and  $x_p$ , are in the forms of

$$x_s = A_s \cdot e^{j\omega t} \text{ and } x_p = A_p \cdot e^{j\omega t} \quad (7)$$

The amplitudes of the displacements,  $A_s$  and  $A_p$ , can be written as

$$\frac{A_s}{\frac{F_0}{K}} = \frac{1 - \frac{\omega^2}{\omega_p^2}}{(1 - \frac{\omega^2}{\omega_p^2}) \cdot (1 + \frac{k}{K} - \frac{\omega^2}{\omega_s^2}) - \frac{k}{K}} \quad (8)$$

and

$$\frac{A_p}{\frac{F_0}{K}} = \frac{1}{(1 - \frac{\omega^2}{\omega_p^2}) \cdot (1 + \frac{k}{K} - \frac{\omega^2}{\omega_s^2}) - \frac{k}{K}} \quad (9)$$

where  $\omega_s = \sqrt{\frac{K}{M}}$  and  $\omega_p = \sqrt{\frac{k}{m}}$  are the resonant frequencies of a TSM sensor and a particle, respectively.

A TSM sensor loaded with a solid particle can be considered as a coupling system based on the mechanical model in Fig. 6. The resonant frequency of this coupling system,  $\omega_c$ , is different from the fundamental resonant frequency of a unloaded TSM sensor,  $\omega_s$ . The relation between,  $\omega_c$ , and,  $\omega_s$ , can be found when the determinant in the right side of (8) becomes zero or the amplitude,  $A_s$ , becomes infinity.

$$(1 - \frac{\omega^2}{\omega_p^2}) \cdot (1 + \frac{k}{K} - \frac{\omega^2}{\omega_s^2}) - \frac{k}{K} = 0 \quad (10)$$

Solve this equation and the resonant frequency of the coupling system,  $\omega_c$ , is given as

$$\omega_{c1,2} = \left( \frac{1}{2} \left[ \left( \frac{k}{m} + \frac{K}{M} + \frac{k}{M} \right) \pm \sqrt{\left( \frac{k}{m} + \frac{K}{M} + \frac{k}{M} \right)^2 - 4 \cdot \frac{k}{m} \cdot \frac{K}{M}} \right] \right)^{1/2} \quad (11)$$

It shows that the resonant frequency of the coupling system,  $f_c = \omega_c / 2\pi$ , is a function of the masses of the TSM sensor,  $M$ , and the coupled object,  $m$ , as well as the spring constants,  $K$  and  $k$ . If the properties of a TSM sensor,  $M$  and  $K$ , are given, by knowing the mass,  $m$ , of the loaded particle, the coupling constant,  $k$ , can be determined from the measurements of the resonant frequency,  $\omega_c$ , of the coupling system. This is very useful in measuring the properties of the interactions between different particles and surfaces in micro and nano scales.

Fig. 7 shows the dependence of the relative change in the resonant frequency,  $\Delta f_c / f_s$ , on the coupling constant,  $k$ , for a TSM sensor loaded with a stainless steel sphere (about 10  $\mu\text{m}$  diameter with mass,  $m$ ). The TSM sensor has a fundamental resonant frequency,  $f_s = 5$  MHz.  $\Delta f_c = f_c - f_s$ , is the change in the resonant frequency of the TSM sensor due to the particle loading.

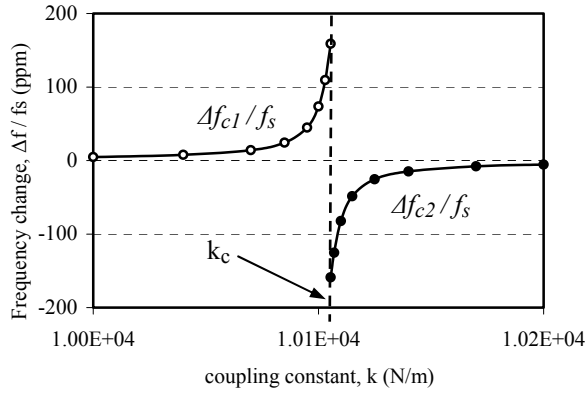


Fig. 7. Relative change in the resonant frequency change,  $\Delta f_c / f_s$ , vs. coupling constant,  $k$

It can be seen that there is a special value for the coupling constant,  $k$ , defined as *critical coupling constant*,  $k_c = m \cdot \frac{K}{M} = m \cdot \omega_s^2 = m \cdot (2\pi f_s)^2$ . This happens when the natural frequency of a particle,  $f_p$ , equals to the fundamental frequency of a TSM sensor,  $f_s$ . At this point,  $k_c$ , maximum frequency changes in the resonant frequency,  $\Delta f_c / f_s$ , are observed.

When  $k$  is larger than  $k_c$ , the resonant frequency of the coupling system,  $f_{c2}$ , is less than the resonant frequency of a unloaded TSM sensor,  $f_s$ . This actually corresponds to the case of a typical mass loading on a TSM sensor, where a decrease in the resonant frequency,  $\Delta f_{c2} = f_{c2} - f_s < 0$ , is measured. This is due to a strong coupling between the

loaded object and the TSM sensor and has been confirmed by many papers [13,14].

If  $k$  is smaller than  $k_c$ , the resonant frequency of the coupling system,  $f_{c1}$ , is greater than  $f_s$ . A weak coupling between the loaded object and the TSM sensor happens and an increase in the resonant frequency,  $\Delta f_{c1} = f_{c1} - f_s > 0$ , is predicted.

When a solid particle is placed on the surface of a TSM sensor, the coupling constant,  $k$ , is not only determined by the properties of the particle and the TSM sensor themselves, such as the resonant frequency of the TSM sensor,  $f_s$ , the roughness of the sensor surface, and the mass of the particle,  $m$ , etc., but also the conditions of the environment, such as the humidity and temperature, etc. This means that the actual coupling constant,  $k$ , between a particle and a TSM sensor may be much different from the critical coupling constant,  $k_c$ . Since a TSM sensor usually has a fixed fundamental resonant frequency, it means that one TSM sensor is only sensitive to a particle at certain coupling conditions.

In Fig. 8 the dependence of the resonant frequency of the coupling system,  $f_c$ , on the coupling constant,  $k$ , is plotted for particles with different diameters.

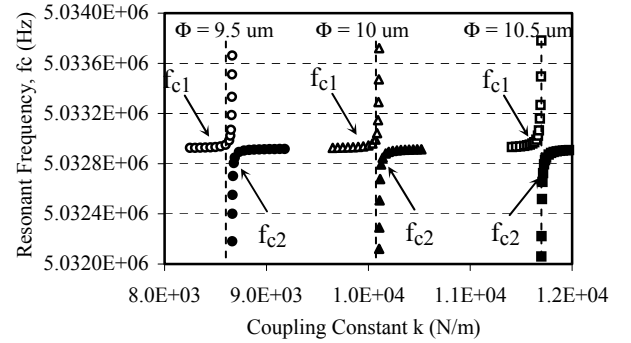


Fig. 8. Resonant frequencies of the coupling system,  $f_c$ , vs. coupling constant,  $k$ , for particles with different diameters

It is clear in Fig. 8 that a small change, about 5% in the diameter or 15% in the mass of a sphere, could significantly change the critical coupling constant for a particle and makes it hard for the same TSM sensor to detect all the three particles. This can be considered as an advantage because the TSM sensor has a high selectivity but at the expense of limited detection range.

### III. Results

#### A. Experimental System

Experiments have been designed to study the interaction between solid particles and the TSM sensor surfaces. Measuring system is shown in Figure 9. A TSM sensor is connected to a HP 4395A Network Analyzer and the frequency response of the scatter matrix is measured.

Based on the changes in the frequency responses of amplitudes and phases due to the particle loading, the properties of the particle can be determined.

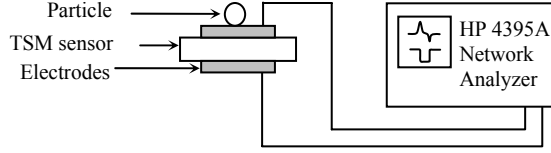


Fig. 9. Measuring system

### B. TSM Sensor Loaded with Stainless Steel Particles

Fig. 10 shows the frequency response of the amplitude of the reflection coefficient,  $S_{21}$ , for a 5 MHz TSM sensor loaded with two stainless steel spheres (30  $\mu\text{m}$  diameter). The resonant frequency of the TSM sensor has an increase of 3 Hz with the particle loading, compared with a resonant frequency decrease for a normal mass or liquid loading.

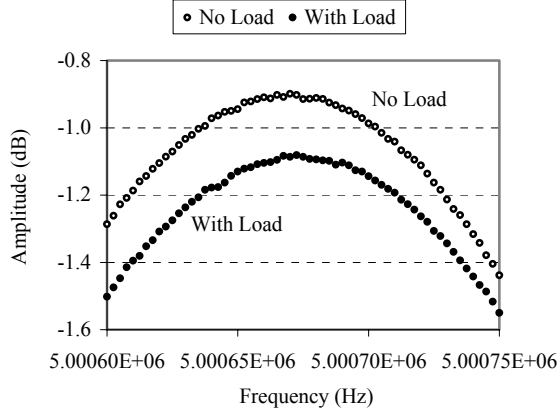


Fig. 10. Amplitude of  $S_{21}$  for a 5 MHz TSM sensor loaded with one stainless steel sphere (30  $\mu\text{m}$ )

The change of the resonant frequency,  $\Delta f_c = f_c - f_s$ , is 3 Hz, or  $\Delta f_c / f_s$  is about 0.6 ppm. Based on the mechanical model presented in the theory part, this corresponds to an interfacial coupling constant,  $k$ , of  $1.08 \times 10^4$  N/m. The result is consistent with the value provided in the reference [2].

As we discussed before, relative large frequency change due to a particle loading only happens when the resonant frequency of a particle is close to the fundamental frequency of a TSM sensor, which is almost fixed after the fabrication of the sensor. Thus a TSM sensor with certain intrinsic frequency is only sensitive to a particle loading within a limited range of diameters. To exploit the sensitivity of a TSM sensor to particles with sizes in a wider range, we have measured the frequency response of a TSM sensor under different environments.

### C. Effect of a Magnetic Field on the Interfacial Interaction

Fig. 11 shows the different frequency responses of the amplitude of the reflection coefficient,  $S_{21}$ , for a TSM

sensor loaded with two stainless steel spheres with and without a magnetic field ( $B = 400$  Gauss).

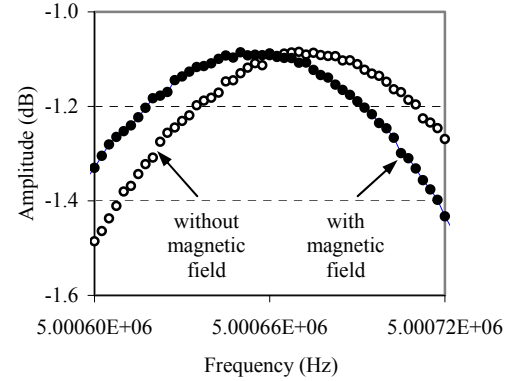


Fig. 11. Frequency response of the amplitude of  $S_{21}$  under magnetic field

It can be seen that the resonant frequency shift is about 12.5 Hz, much larger than the 3 Hz change measured without magnetic field as it is seen in Fig. 10. This result not only helps to understand the effect of a magnetic field on the interfacial interaction between particles and a surface, but also increases the measurand or sensitivity of a TSM sensor. Therefore, a wider size range for particle loadings can be expected.

Fig. 12 shows the responses of a TSM sensor to removals of a single particle. A 5 MHz TSM sensor was loaded with seven stainless steel spheres with sizes of 30  $\mu\text{m}$ . After a magnetic field ( $B = 400$  Gauss) was applied, a single sphere was removed successively except the last step where two spheres were removed. An averaged frequency shift of 5 Hz was observed for the removal of a single sphere and 10 Hz for the removal of two spheres.

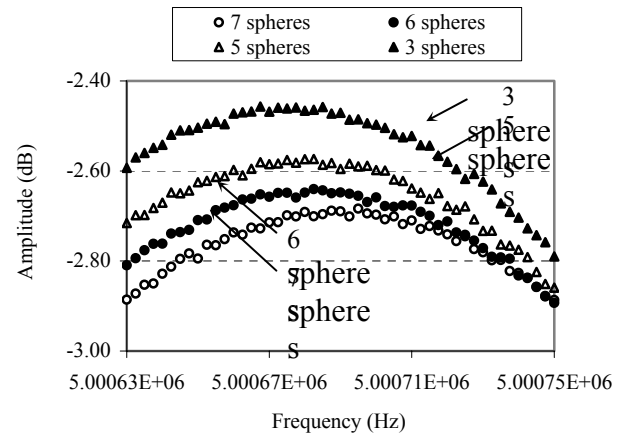


Fig. 12. The changes on the amplitude of  $S_{21}$  under magnetic field when subsequent particles are removed

## IV. SUMMARY

In this paper we present a preliminary study of the interfacial interaction between a solid particle and a solid surface using TSM sensors. The main sources contributing

to the interaction, such as Van der Waals force and gravitational force, have been discussed and a mechanical model has been developed. A frequency increase for a solid particle loading has been predicted and verified by experiments. It has been shown that the coupling constant,  $k$ , is very sensitive to the interfacial interaction and this important value can be determined based on the measurement of the change in the resonant frequency of a TSM sensor and the proposed mechanical model.

Effect of a magnetic field on the interaction has been experimentally evaluated. The results have indicated potential methods to change the strength of the interfacial interactions between solid particles and surfaces.

It has been shown that the TSM sensor technique can provide information of the interaction between solid particles and surfaces.

## Reference:

- [1] J. N. Israelachvili, Intermolecular and surface forces, 2<sup>nd</sup> Edition, Academic Press, 1992.
- [2] G. L. Dybwad, A sensitive new method for the determination of adhesive bonding between a particle and a substrate, *J. Appl. Phys.* 58 (7), pp.2789-2790, Oct. 1985.
- [3] A. Torii, M. Sasaki, K. Hane, and S. Okuma, Adhesive Force of the microstructures measured by the Atomic Force Microscope, pp.111-116, 1993.
- [4] M. Sitti, and H. Hashimoto, Force controlled pushing of nanoparticles: modeling and experiments, *Proceedings of the 1999 IEEE/ASME International Conference on Advanced Intelligent Mechantronics*, pp. 13- 20, September 1999.
- [5] H. Hashimoto, and M. Sitti, Challenge to micro-nanomanipulation using Atomic Force Microscope, *International Symposium on MicroMechatronics and Human Science*, pp.35-42, 1999.
- [6] A. L. Weisenhorn, P. Maivald, H. J. Butt, and P. K. Hansma, Measuring adhesion, attraction, and repulsion between surface in liquids with an Atomic-Force Microscope, *Physical Review B*, Vol. 45, No. 19, pp.11226-11232, 1992.
- [7] S. Tombelli, M. Mascini, C. Sacco, and A. P. F. Turner, A DNA piezoelectric biosensor assay coupled with a polymerase chain reaction for bacterial toxicity determination in environmental samples, *Analytica Chimica Acta*, vol.418, pp.1-9, Aug., 2000
- [8] K. Barbee, K. Sun, R. M. Lec, and J. Sorial, The study of a cell-based TSM piezoelectric sensor, *Proceedings of 2002 IEEE International Frequency Control Symposium and PDA Exhibition*, Page(s): 260 –267, 2002.
- [9] D. McMullan, *Scanning Electron Microscopy 1928–1965*, *SCANNING* Vol. 17, 175–185, 1995.
- [10] J. E. Griffith, G. E. Kochanski, *Scanning Tunneling Microscopy*, *Annu. Rev. Mater. Sci.* vol.20, pp.219-244, 1990
- [11] G. Binnig, C. F. Quate, and Ch. Gerber, Atomic force microscope. *Phys. Rev. Lett.*, 56 (9), pp. 930-933, 1986
- [12] Lec, R. M., Piezoelectric biosensors: recent advances and applications, *Proceedings of 2001 IEEE International Frequency Control Symposium and PDA Exhibition*, pp. 419 –429, 2001.
- [13] G. Z. Sauerbrey, *Physics*, vol.155, pp.206-222, 1959.
- [14] P. L. Konash and G. J. Batiaans, *Anal. Chem.* 52, pp. 1929, 1980.
- [15] C. E. Reed, K. K. Kanazawa, and J.H. Kaufman, Physical Description of A Viscoelastically Loaded AT-cut Quartz Resonator, *J. Appl. Phys.* 68 (5), pp. 1993-2001, 1990.
- [16] B. Drafts, *Acoustic Wave Technology Sensors*, *IEEE Trans. Microwave Theory and Techniques*, vol. 49, no. 4, pp. 795-802, April, 2001.
- [17] E. Benes, Improved Quartz Crystal Microbalance Technique, *J. Appl. Phys.* 56 (3), pp. 608-626, 1984
- [18] S. J. Martin, V. E., and G. C. Frye, Characterization of A Quartz Crystal Microbalance with Simultaneous Mass and Liquid Loading, *Anal. Chem.* (63), pp.2272-2281, 1991.